# Effect of Polymer Composition on Polymer Diffusion in Poly(butyl acrylate-*co*-methyl methacrylate) Latex Films

**Yuanqin Liu,† Jeffrey C. Haley,† Kangqing Deng,† Willie Lau,‡ and Mitchell A. Winnik*,†**

*Department of Chemistry, University of Toronto, 80 St. George Street, Toronto, Ontario M5S 3H6, and Rohm and Haas Company, 727 Norristown Road, Spring House, Pennsylvania 19477*

*Received April 11, 2007; Revised Manuscript Received June 8, 2007*

ABSTRACT: We describe polymer diffusion measurements in poly(butyl acrylate-*co*-methyl methacrylate) [P(BA−MMA)] copolymer latex films by fluorescence resonance energy transfer (FRET). Four sets of copolymers were prepared from various weight ratios of butyl acrylate and methyl methacrylate by semicontinuous emulsion polymerization. Their glass transition temperatures range from 4 to 28 °C. Latex particles were labeled with phenanthrene (Phe) as the donor dye and with 4-(*N*,*N*-dimethylamino)benzophenone (NBen) as the acceptor dye. Latex films were cast from a 1:1 mixture of Phe- and NBen-labeled latex samples. Polymer diffusion was monitored as a function of annealing temperature, and apparent diffusion coefficients ($D_{app}$) were calculated from the energy transfer data using a simple diffusion model. These values increased with annealing temperature and decreased with $T_g$. Rheology measurements recorded the response of the dynamic moduli ($G'$, $G''$) with respect to oscillatory shear frequency ($\omega$) over a range of temperature close to that of the diffusion experiments. The temperature dependence of polymer dynamics extracted by the rheology experiments is in good agreement with the temperature dependence of $D_{app}$. Increasing the BA copolymer content leads to an apparent increase in long-chain branching, which is reflected in both the time dependence of $D_{app}$ and in the dynamic moduli measurements. A greater degree of branching leads to a broader distribution of polymer diffusion coefficients and a stronger time dependence of $D_{app}$.

## Introduction

Environmental considerations are driving changes in the coatings industry.[1] One important change is the replacement of solvent-based paints with waterborne (latex) paints. Latex paints, however, still contain significant amounts of volatile organic solvents (VOCs).[2] These solvents serve as fugitive plasticizers: They soften the particles so that the forces associated with drying are sufficient to deform the spherical latex particles into polyhedral cells that form a continuous and void-free film. They enhance the rate of the diffusion of polymer molecules across the boundaries between these cells. This is the step that leads to the development of good mechanical properties of the latex film. At this time the polymer film is often soft and tacky. Over time, these VOCs evaporate from the film, increasing its glass transition temperature and its hardness at room temperature.

New knowledge is needed to develop latex coatings that do not require VOCs and which have similar or enhanced performance properties to current technology. As a step in this direction, we have undertaken a study of polymer diffusion in films formed from a series of latex consisting of butyl acrylate−methyl methacrylate−methacrylic acid (BA−MMA−MAA) copolymers of different compositions. These acrylic latex are widely used in architectural coatings (house paints). Typical coatings in current use consist of BA/MMA weight ratios of 50/49 with 1 wt % MAA. Increases in the BA content decrease the glass transition temperature ($T_g$) of the latex polymer, which should lead to a smaller requirement for added solvent. In the study reported below, we explore how the composition of the latex polymer affects the rate of polymer diffusion (and its temperature dependence) for a series of BA/MMA latex containing 1 wt % MAA, all with polymers of very similar molar mass. These polymer diffusion rates were studied using the fluorescence resonance energy transfer (FRET) methods developed in our laboratory.[3] The influence of temperature on the diffusion rates was correlated with the results of rheology measurements on samples of the same composition.

Increasing BA content in the latex has two effects on the polymer diffusion process. First, it reduces $T_g$. In addition, increased BA content leads to changes in the polymer diffusion rates and rheological behavior beyond those expected from the change in $T_g$. These changes can be explained by increases in the extent of long-chain branching along the polymer backbone. This branching increase leads to a large broadening of the distribution of polymer diffusion coefficients in the system. This result has important implications for low VOC BA/MMA latex coatings.

## Experimental Section

**Materials.** Potassium persulfate (KPS), sodium carbonate ($Na_2CO_3$), and 1-dodecanethiol ($C_{12}$-SH) were used as received from Aldrich. Polystep A-16 (22% solution of dodecylbenzene and tridecylbenzenesulfonates,[1] Stepan Co., Maywood, NJ) and methyl-$\beta$-cyclodextrin were kindly supplied by Rohm and Haas Co. and used as received. Methyl methacrylate (MMA, Aldrich), butyl acrylate (BA, Aldrich), and methacrylic acid (MAA, Aldrich) were distilled at reduced pressure, and the purified monomers were stored at 0 °C until use. Water was purified by a Milli-Q ion-exchange filtration system. Phenanthrylmethyl methacrylate (PheMMA) was used as received from Toronto Research Chemicals Inc. 4′-Dimethylamino-2-methacryloxy-5-methylbenzophenone (NBenMA) was synthesized as described elsewhere.[4,5]

**Latex Preparation.** All latex dispersions were prepared by semicontinuous emulsion polymerization reactions. A typical recipe for the synthesis of nonlabeled P(BA−MMA) (BA:MMA weight ratio 60:39) latex is shown in Table 1. In the first stage, a dispersion of seed particles was prepared by batch emulsion polymerization

† University of Toronto.
‡ Rohm and Haas Company.

10.1021/ma070853c CCC: $37.00 
Published on Web 07/27/2007

**Table 1. Typical Recipe for the Synthesis of Nonlabeled $P(BA_{60}-MMA_{39})^a$ Latex**

| ingredients (g) | first stage | second stage |
|---|---|---|
| $H_2O$ | 3.0 | |
| Polystep A-16[b] | 0.13 | |
| methyl-$\beta$-cyclodextrin | 0.13 | |
| $Na_2CO_3$ | 0.05 | |
| KPS | 0.06 | 0.01 |
| monomer preemulsion | 0.44 | 14.25 |
| $H_2O$ | 4.5 | |
| Polystep A-16 | 0.16 | |
| BA | 6.0 | |
| MMA | 3.9 | |
| MAA | 0.1 | |
| $C_{12}$-SH[c] | 0.025 | |

[a] The subscripts refer to the wt % of each monomer. All latex samples contain 1 wt % MAA. [b] 22 wt % surfactant solution, primarily sodium dodecylbenzenesulfonate. [c] 1-Dodecanethiol, chain transfer agent, used at 0.25 wt % of total monomers.

with 3 wt % of a preemulsion of monomers, surfactant, chain transfer agent, and water. Water (3.0 g), Polystep A-16 (0.13 g), and Me-$\beta$-CD (0.13 g) were added in a 100 mL three-neck flask equipped with a mechanical stirrer, nitrogen inlet, and condenser. The flask was immersed in an oil bath. The system was thoroughly purged with nitrogen while the reaction mixture was heated to 80 °C. After the reactor temperature stabilized at 80 °C, the KPS solution (0.06 g in water 0.5 g) as an initiator and the $Na_2CO_3$ solution (0.05 g in water 0.5 g) as a pH buffer were added into the reactor followed by the addition of 3 wt % of monomer preemulsion (0.44 g). The mixture was stirred for 20 min at 80 °C.

In the second stage of polymerization, the remaining monomer preemulsion was fed into the seed latex dispersion together with an initiator aqueous solution (0.01 g in water 2.0 g). The monomer feeding rate was kept constant (0.1 mL/min), controlled by Fluid Metering QG50 pumps, with a total feeding time of 3 h. After the addition was completed, the system was maintained at 80 °C for 0.5 h. Then the reaction was cooled to room temperature. A latex dispersion with ca. 50 wt % solids content was produced. The particle size is about 150 nm in diameter with a narrow size distribution.

Fluorescence dye-labeled latex samples were synthesized in a similar fashion. For the donor-labeled particles, 1 mol % PheMMA (based on total monomer) was added into the monomer preemulsion. For the acceptor labeled particles, 0.3 mol % NBenMA (based on total monomer) was added into the monomer preemulsion. The characteristics of these latex samples are listed in Table 2.

**Characterization of Latex Particles.** Particle diameters were measured by dynamic light scattering at a fixed scattering angle of 90° at 23 °C with a Brookhaven Instruments model BI-90 particle sizer equipped with a 10 mW He−Ne laser. Particle sizes and size distributions were also measured by capillary hydrodynamic fractionation using a MATEC model 2000 CHDF. The solids content of each latex dispersion was determined by gravimetry. Polymer molecular weight and polydispersity index (PDI) were measured by gel permeation chromatography (GPC) using a Viscotek liquid chromatograph equipped with a Viscotek model 2501 UV detector and a Viscotek TDA302 triple detector. Two Viscotek GMHHR Mixed Bed columns were used with tetrahydrofuran (THF) as the elution solvent at a flow rate of 0.6 mL/min. Polystyrene standards were used for calibration. The glass transition temperature ($T_g$) of copolymers was measured with a TA Instruments DSC Q100 V7.3 Build 249 differential scanning calorimeter over a temperature range of −50 to 150 °C at a heating rate of 10 °C/min. Each sample was taken through two runs. $T_g$ values were calculated from the second run, and the values determined are shown in Table 2.

Gel content was measured by the centrifugation method developed in our laboratory:[6] A latex sample (1.0 g) was dried to a constant weight $W_0$. The dried polymer was subsequently immersed in tetrahydrofuran (THF, 10 mL). The mixture was agitated gently at room temperature for 24 h. The resulting solution was then centrifuged at 20 000 rpm for 30 min, and the top transparent layer was poured off. When gel was present, a precipitate remained. The precipitate was washed three more times with excess THF to remove residual sols from the gel. The remaining sample (the gel fraction) was dried and weighed ($W_1$). The gel content (%) was calculated from the equation

$$\text{gel content (\%)} = (W_1/W_0) \times 100 \tag{1}$$

**Film Formation and Fluorescence Decay Measurements.** Latex films for energy-transfer experiments were prepared from a 1:1 particle mixture of the donor- and acceptor-labeled dispersions. Several drops of a latex dispersion (about 50 wt % solids content) was spread on a small quartz plate (20 × 8 mm). The film was allowed to dry uncovered in a refrigerator at 4 °C to minimize polymer interdiffusion during the drying process. The film was dry within 1 h. The films prepared in this way have a thickness of ca. 60 $\mu$m. Films were transparent for $P(BA_{60}-MMA_{39})$, $P(BA_{55}-MMA_{44})$, and $P(BA_{50}-MMA_{49})$ latex but turbid for $P(BA_{40}-MMA_{59})$ samples due to its high $T_g$. Solvent-cast films were prepared from the same polymer mixture. A latex film was allowed to dry, and the dry film was dissolved in a small amount of THF. Then the solution was cast onto a small quartz plate and allowed to dry at room temperature for 24 h.

The films on quartz plates were placed directly on a high mass (2 cm thick) aluminum plate in an oven preheated to the annealing temperature and then annealed for various periods of time. Under these conditions, we estimate that it takes less than 1 min for the film to reach the preset oven temperature. The annealed films were taken out of the oven and placed directly on another high mass aluminum plate at 4 °C for 2 min before carrying out fluorescence decay measurements. Fluorescence decay profiles of the films at 23 °C were measured by the time-correlated single photon counting technique[7] using a nanosecond time-correlated single photon counting system from IBH with a NanoLED ($\lambda_{ex}$ = 296 nm) as the excitation source. Each film was placed in a quartz tube for the measurement. The emission was collected from 335 to 366 nm. A 335 nm cutoff filter was mounted in front of the emission monochromator (350 ± 16 nm) to minimize the amount of scattered light from the sample entering the detector. Data were collected until 5000 counts were accumulated in the maximum channel, and these data were fitted by nonlinear least-squares using the delta function convolution method.[7] The instrumental response function was obtained by using a degassed *p*-terphenyl solution (0.96 ns lifetime) as a mimic standard.[8]

**Data Analysis.** In the absence of benzophenone as an energy-transfer acceptor, for all samples containing 1 mol % donor, the phenanthrene decay profiles were exponential, with lifetime $\tau_D$ = 44.3 ns. The goodness-of-fit parameter (chi-square) for these single-exponential fits ranged from 1.01 to 1.10. In the presence of an energy-transfer acceptor, the fluorescence decay curves became nonexponential. The shape of the curve depends on the details of the donor−acceptor (D/A) pair distribution. In a system with uniformly distributed donors and acceptors in three dimensions in the absence of diffusion, the donor fluorescence intensity decay $I_D(t)$ following instantaneous excitation is described by the Förster equation:[9]

$$I_D(t) = A \exp\left[-\frac{t}{\tau_D} - P\left(\frac{t}{\tau_D}\right)^{1/2}\right] \tag{2}$$

where

$$P = \frac{4}{3}\pi^{3/2}\left(\frac{3}{2}\langle\kappa^2\rangle\right)^{1/2} N_A R_0^3 [Q] \tag{3}$$

Here, [Q] is the concentration of acceptor (quencher), and $P$ is proportional to [Q]. $R_0$ is the critical Forster radius for energy transfer. $N_A$ is Avogadro's number. The orientation factor $\langle\kappa^2\rangle$ describes the average orientation of dipoles of donor and acceptor

**Table 2. Characteristics of the Latex Polymers and Particles**

| latex sample name | $M_n$ | PDI | $T_g$ (°C) | $d^a$ (nm) | $d_n{}^b$ (nm) | $d_w/d_n{}^b$ | solids content (%) |
|---|---|---|---|---|---|---|---|
| P($BA_{60}$−$MMA_{39}$) | 31 000 | 3.7 | 4 | 151 | 156 | 1.1 | 48.2 |
| Phe-P($BA_{60}$−$MMA_{39}$) | 31 000 | 3.1 | | 156 | 166 | 1.1 | 44.2 |
| NBen−P($BA_{60}$−$MMA_{39}$) | 29 000 | 2.1 | 3 | 141 | 159 | 1.3 | 54.1 |
| P($BA_{55}$−$MMA_{44}$) | 48 000 | 2.9 | 7 | 152 | 159 | 1.2 | 44.3 |
| Phe−P($BA_{55}$−$MMA_{44}$) | 47 000 | 3.0 | | 151 | 163 | 1.0 | 43.1 |
| NBen−P($BA_{55}$−$MMA_{44}$) | 46 000 | 2.8 | 7 | 157 | 142 | 1.1 | 41.1 |
| P($BA_{50}$−$MMA_{49}$) | 50 000 | 2.0 | | 170 | 150 | 1.2 | 42.3 |
| Phe-P($BA_{50}$−$MMA_{49}$) | 45 000 | 2.7 | 12 | 159 | 146 | 1.1 | 40.2 |
| NBen−P($BA_{50}$−$MMA_{49}$) | 43 000 | 2.2 | | 191 | 203 | 1.1 | 45.7 |
| P($BA_{40}$−$MMA_{59}$) | 51 000 | 2.0 | | 148 | 152 | 1.3 | 47.6 |
| Phe−P($BA_{40}$−$MMA_{59}$) | 44 000 | 2.1 | 28 | 147 | 155 | 1.1 | 29.4 |
| NBen−P($BA_{40}$−$MMA_{59}$) | 41 000 | 3.7 | 27 | 152 | 151 | 1.2 | 52.0 |

[a] Data for the particle diameter $d$ from the BI-90 particle sizer. [b] Number-average $d_n$ and weight-average $d_w$ diameter data from the CHDF 2000 (MATEC).

molecules. $\langle\kappa^2\rangle$ has a value of 2/3 in fluid solution, where rotation is rapid. It takes a value of $\langle\kappa^2\rangle = 0.476$ for a random distribution of immobile chromophores in three dimensions, a situation typical of dyes in polymer matrices.[10]

To obtain an accurate area for each decay profile, we fitted each decay curve to the empirical equation (4) and then evaluated the integral analytically from the magnitude of the fitting parameters.

$$I_D(t) = A_1 \exp\left[-\frac{t}{\tau_D} - P\left(\frac{t}{\tau_D}\right)^{1/2}\right] + A_2 \exp\left(-\frac{t}{\tau_D}\right) \qquad (4)$$

From the calculated area data we can calculate the quantum efficiency of energy transfer $\Phi_{ET}(t_n)$ for samples aged or annealed for a time $t_n$

$$\Phi_{ET}(t_n) = 1 - \frac{\int_0^\infty I_{DA}(t)\,dt}{\int_0^\infty I_D(t)\,dt} = 1 - \frac{\text{area}(t_n)}{\tau_D} \qquad (5)$$

where $I_{DA}(t)$ and $I_D(t)$ refer to the normalized decay functions of donor fluorescence intensity in the D/A film and in the donor only film, respectively. Because the unquenched donor decay profile here is exponential, its integral is equal the unquenched donor lifetime $\tau_D$.

The "extent of mixing" parameter $f_m$ is a useful measure of the extent of polymer interdiffusion

$$f_m(t_n) = \frac{\Phi_{ET}(t_n) - \Phi_{ET}(0)}{\Phi_{ET}(\infty) - \Phi_{ET}(0)} = \frac{\text{area}(0) - \text{area}(t_n)}{\text{area}(0) - \text{area}(\infty)} \qquad (6)$$

This parameter depicts the fractional growth of energy transfer in the D/A films. $\Phi_{ET}(0)$ refers to the extent of energy transfer across the particle boundaries in the newly formed film, whereas $\Phi_{ET}(\infty)$ represents the energy transfer efficiency in a fully mixed D/A film, in which the donors and acceptors are randomly distributed. $\Phi_{ET}(t_n)$ is the degree of energy transfer in a film annealed for time $t_n$.

**Rheology Measurements.** The viscoelastic response of P(BA−MMA) samples was studied at several temperatures above $T_g$ with a Rheometrics RAA instrument in the oscillatory shear mode. We employed a pair of parallel plates (25 mm diameter). The frequency was scanned between 0.01 and 100 rad/s at a constant temperature. Strain sweeps were employed to ensure that all measurements were made in the linear viscoelastic regime. The range of temperatures studied was selected to be as close as possible to the range of temperature used in the energy transfer experiments performed on these materials. However, the lowest temperatures used are limited by the sample modulus at temperatures close to $T_g$.

The following procedure was used to prepare the samples for the measurements of viscoelastic properties. First, the samples were dried under vacuum at 40 °C for 12 h to eliminate any trace of volatiles. Then, the samples were pressed between cleaned polytetrafluoroethylene (PTFE) sheets in a Carver press at 100 °C to eliminate air bubbles. The thickness of the samples was controlled using separators between the plates of the press. In this way, samples free of bubbles, approximately 25 mm in diameter and 1 mm thick, were obtained.

## Results

**Preparation and Characterization of the Latex Samples.** Poly(butyl acrylate-*co*-methyl methacrylate) [P(BA−MMA)] was used as the base copolymer in our diffusion study. All latexes were prepared by semicontinuous emulsion polymerization. In previous work in our laboratory, in order to obtain similar size donor- and acceptor-labeled particles, we used the same unlabeled seeds particles for the synthesis of both the donor- and acceptor-labeled latex, and the polymerizable dye derivative was added only in the second stage.[4,11] This is an easy and efficient way to control particle size. These seeds represent ca. 8−10 wt % of the final latex particles. If the seed particles are prepared by batch emulsion polymerization, they normally have a higher molar mass and broader PDI than the second stage polymer. To some extent, this may lead to a nonuniform dye distribution in the particles. We have always treated this as a minor problem.

Nevertheless, in order to overcome the disadvantage of preformed nonlabeled seeds, we used an in-situ seeding process in the experiments described here. While this is common practice in industry for large-scale reactions, this is a skill-testing challenge for emulsion polymerization reactions run on the small scale (10 g of total monomers) we employ to synthesize labeled latex. On a small scale, slight variations in particle nucleation can have large consequences for particle size and size distribution. One can also experience problems in matching the polymer molar mass and PDI between samples. The challenge for us, which in the past led to our use of common unlabeled seeds, was the need for the donor- and acceptor-labeled particles to have similar diameters and contain polymers of similar $M_n$ and PDI. For the latex samples described here, we employed the same monomer preemulsion containing: monomers, dye comonomers, surfactant, chain transfer agent, and water for making the seed particles in the first stage and for particle growth in the second stage as well. These reactions worked well, and we were able to achieve reasonable control over particle size and polymer molar mass, not only for D- and A-labeled particles of a given composition but also for the entire series of latex examined here.

All emulsion polymerizations contained 1 wt % of MAA. In commercial latex, small amounts of methacrylic acid are normally employed to enhance the colloidal stability of the latex. We follow this practice here. The four pairs of samples we synthesized had monomer weight ratios of BA:MMA:MAA of 60:39:1, 55:44:1, 50:49:1, and 40:59:1. These copolymers are

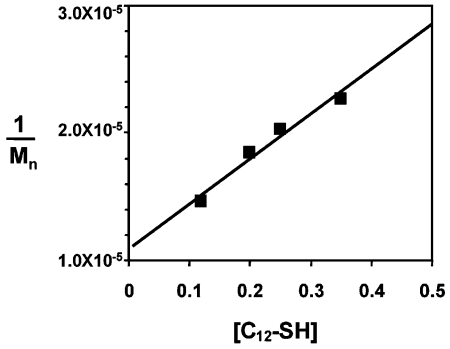


**Figure 1.** Plot of $1/M_n$ against concentration of $C_{12}$-SH of P($BA_{60}$−$MMA_{39}$) latex samples.

named according to their BA:MMA compositions as P($BA_{60}$−$MMA_{39}$), P($BA_{55}$−$MMA_{44}$), P($BA_{50}$−$MMA_{49}$), and P($BA_{40}$−$MMA_{59}$). The glass transition temperatures ($T_g$) of the copolymers were measured by DSC, giving $T_g$ ca. 4 °C for P($BA_{60}$−$MMA_{39}$), 7 °C for P($BA_{55}$−$MMA_{44}$), 12 °C for P($BA_{50}$−$MMA_{49}$), and 27 °C for P($BA_{40}$−$MMA_{59}$). All values are similar to those estimated values from the Fox equation using $T_g$(PBA) = −47 °C and $T_g$(PMMA) = 105 °C.

Dodecyl mercaptan ($C_{12}$-SH) was added in the emulsion polymerization reactions as a chain-transfer agent both to control the molecular weight and to limit or suppress gel formation. Our target in these studies was to obtain high molar mass with very low gel content. This will serve as a baseline for future experiments with latex comprised of lower molar mass polymer. In order to optimize the reaction conditions, a series of P($BA_{60}$−$MMA_{39}$) latex samples were prepared in the presence of various amounts of $C_{12}$-SH. The latex polymer samples obtained were analyzed by GPC. As shown in Figure 1, the plot of $1/M_n$ against [$C_{12}$-SH] was linear, indicating that in the presence of $\beta$-cyclodextrin $C_{12}$-SH provides good control over polymer molar mass. When the amount of $C_{12}$-SH in the reaction was 0.25 wt % based on monomer in the preemulsion, the polymers obtained had less than 5% gel; with lower amounts of chain transfer agent, the latex formed had a significant gel content. Thus, all the latex samples used in the diffusion experiments were prepared in the presence of 0.25 wt % $C_{12}$-SH. The characteristics of all of the latex particles synthesized are summarized in Table 2. The $M_n$ values were in the range of 30 000−50 000 with a PDI between 2 and 3.7. Comparing $M_n$ of the dye-labeled and nonlabeled latex polymers, we infer that the dye monomer did not significantly affect the polymerization reaction.

The proton NMR spectra of the four different latex polymer compositions are compared in Figure 2. From the ratio of integrals of peaks a and b, which correspond to protons at position a and b, respectively, we calculated the mole ratios of BA:MMA were 1.5:1.0 for P($BA_{60}$−$MMA_{39}$), 1.1:1.0 for P($BA_{55}$−$MMA_{44}$), 0.8:1.0 for P($BA_{50}$−$MMA_{49}$), and 0.5:1.0 for P($BA_{40}$−$MMA_{59}$); the weight ratios of BA:MMA were 65:35 for P($BA_{60}$−$MMA_{39}$), 58:42 for P($BA_{55}$−$MMA_{44}$), 51:49 for P($BA_{50}$−$MMA_{49}$), and 41:59 for P($BA_{40}$−$MMA_{59}$). These results indicate that the composition of the polymers closely resembled the monomer feed composition in our emulsion polymerization reactions under monomer-starved conditions. The particle size and size distribution were characterized by both right-angle dynamic light scattering and by CHDF. As shown in Table 2, all samples have particle diameters of ca. 150 nm. For all latex samples the $d_w/d_n$ values obtained by CHDF are less than 1.3, which indicates a narrow size distribution.

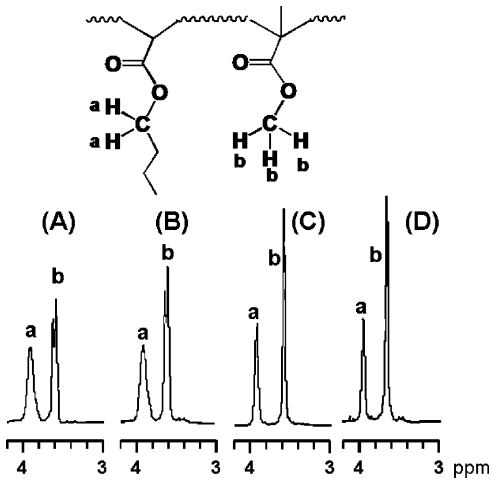


**Figure 2.** $^1$H NMR spectra of (A) P($BA_{60}$−$MMA_{39}$), (B) P($BA_{55}$−$MMA_{44}$), (C) P($BA_{50}$−$MMA_{49}$), and (D) P($BA_{40}$−$MMA_{59}$). $CDCl_3$ was used as solvent. Peaks a and peak b correspond to protons at positions a and b, respectively.

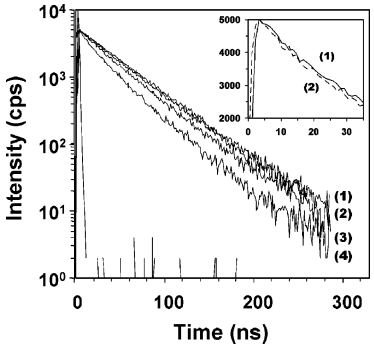


**Figure 3.** Phenanthrene (donor) fluorescence decay curves [$I_D(t)$] measured at 23 °C for Phe−P($BA_{60}$−$MMA_{39}$) latex films: (1) Phe-labeled latex only, (2) a newly formed film dried at 4 °C, consisting of a 1:1 ratio of Phe−P($BA_{60}$−$MMA_{39}$) and NBen−P($BA_{60}$−$MMA_{39}$), (3) the same film as in (2) aged for 47 min at 23 °C, and (4) a solvent-cast film from a 1:1 mixture of the two freeze-dried polymers dissolved in THF and then annealed at 120 °C for 2 h. Note that curves (1) and (2) overlap. The inset shows curves (1) and (2) at short times on a linear scale.

**Energy-Transfer Studies of Polymer Diffusion.** Films for FRET experiments were prepared from a 1:1 mixture Phe- and NBen-labeled latex particles. Several drops of the latex mixture was cast onto a small quartz plate (20 × 8 mm) and allowed to dry in a refrigerator at 4 °C over 1 h. The film thicknesses were ca. 60 $\mu$m. The films obtained from P($BA_{60}$−$MMA_{39}$), P($BA_{55}$−$MMA_{44}$), and P($BA_{50}$−$MMA_{49}$) D/A mixtures were transparent and free of cracks. However, the films prepared from P($BA_{40}$−$MMA_{59}$) latex were turbid and showed some cracks even if they were dried at 23 °C. We attribute this behavior to the high minimum film formation temperature (MFT) of this sample caused by the high $T_g$ of the latex polymers. Freshly formed latex films were transfer to the sample chamber of the fluorescence decay instrument in a cold quartz tube, and fluorescence decays were measured immediately. This whole process took less than 2 min. The films were then annealed in a preheated oven for various periods of time at certain temperatures. The fluorescence decays were monitored as a function of annealing time at a series of temperatures.

Figure 3 shows representative donor fluorescence decays for a donor-labeled P($BA_{60}$−$MMA_{39}$) latex film [curve (1)] and a D/A mixed P($BA_{60}$−$MMA_{39}$) latex film aged for various periods of time at room temperature (23 °C) [curves (2−3)]. The decay curve (1) in Figure 3 is exponential with a lifetime of 44.3 ns.

Films of the donor-labeled P($BA_{60}$−$MMA_{39}$) latex with the other three BA−MMA compositions gave the same lifetimes. For these polymers, we see that the donor lifetime is independent of polymer composition. Curve (2) in Figure 3 is the decay profile of a newly formed film from a 1:1 D/A mixture. It is not exponential, but the deviation at early times is small (shown in Figure 3 inset) because very little polymer diffusion has occurred. We assume that the major contribution to the curvature of this plot is energy transfer across the particle boundary. From the decays of a series of similar films, we calculate quantum efficiency of energy transfer ($\Phi_{ET}$) of 0.06−0.07 in newly formed films using eq 5. We take 0.06 as the value of $\Phi_{ET}(0)$. Curve (3) in Figure 3 depicts the decay profile of the film in curve (2) after 47 min aging at 23 °C. The increased curvature at early decay times is an indication that some polymer diffusion has taken place, resulting in an increase in $\Phi_{ET}$.

Curve (4) in Figure 3 shows much more pronounced curvature. It represents the decay profile for a film cast from a THF solution. In solvent-cast films, the donor- and acceptor-labeled polymers may be thought of as randomly mixed in solution, but can undergo some demixing upon drying, due to correlation hole effects. We refer to the $\Phi_{ET}$ value obtained from solvent-cast films as $\Phi_{ET}$(lim). It represents the limiting maximum value of $\Phi_{ET}$ that could be obtained from diffusive mixing. This value can be smaller than, but is often equal to, $\Phi_{ET}(\infty)$, the value corresponding to complete randomization of the dyes in the system. For latex films formed from linear polymers, $\Phi_{ET}$(lim) and $\Phi_{ET}(\infty)$ are commonly very similar in magnitude, but in latex films consisting of highly branched polymers or polymer with a significant gel content, $\Phi_{ET}$(lim) $< \Phi_{ET}(\infty)$.

Values of $\Phi_{ET}(\infty)$ were determined in a series of model experiments in which samples of each of the Phe-labeled polymers were mixed with different amounts of NBenMA as a low molar mass acceptor. Films were prepared by solvent-casting, and $I_D(t)$ decay profiles were measured. Individual decays were fitted to eq 2, and values of the fitting parameter $P$ were plotted against [NBenMA] (Figure S4 in the Supporting Information). These plots were linear and for each polymer led to a value of $R_0 = 2.5$ nm, consistent with the value reported previously.[5] From this value and the composition of the 1:1 Phe/NBen latex films, we calculated values of $\Phi_{ET}(\infty) = 0.50$. We used this value in all of our calculations of $f_m$ (eq 6).

**Polymer Diffusion in P($BA_{60}$−$MMA_{39}$) Films at Different Temperatures.** A series of Phe- and NBen-labeled P($BA_{60}$−$MMA_{39}$) latex films were cast at 4 °C and dried for 1 h. The films were annealed at various temperatures, and their fluorescence decay curves were measured at different periods of annealing time. From the newly formed films we found the quantum efficiency before annealing, $\Phi_{ET}(0) = 0.06-0.07$. The maximum $\Phi_{ET}$ value was obtained from fully mixed D/A films which were cast from a THF solution of 1:1 Phe- and NBen-labeled P($BA_{60}$−$MMA_{39}$) polymers. The $\Phi_{ET}$ value for this newly formed solvent cast film was 0.42. Annealing this film at 120 °C for 2 h lead to a decrease of the $\Phi_{ET}$ value to 0.38, and there was no additional decrease with further annealing. We take $\Phi_{ET}$(lim) = 0.38.

The calculated $\Phi_{ET}$ values are plotted against annealing time in Figure 4A for experiments at different temperatures ranging from 23 to 90 °C. The curves show a large increase in $\Phi_{ET}$ values at early stages and a smaller increase at longer times. The plot shows that $\Phi_{ET}$ has a strong temperature dependence. From 23 to 90 °C, not only the plateau $\Phi_{ET}$ values but also the growth rate of $\Phi_{ET}$ increased significantly. Since we know that

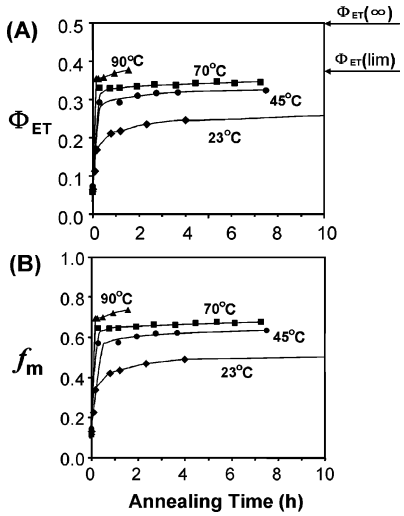


**Figure 4.** Plots of $\Phi_{ET}$ (A) and $f_m$ (B) vs annealing time for the P($BA_{60}$−$MMA_{39}$) latex films annealed at 23, 45, 70, and 90 °C.

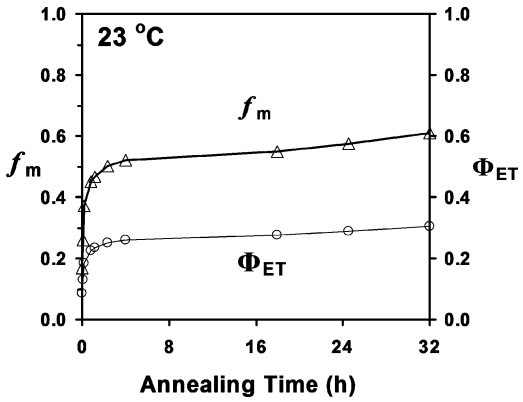


**Figure 5.** Plots of $\Phi_{ET}$ and $f_m$ vs annealing time for the P($BA_{60}$−$MMA_{39}$) latex films annealed at 23 °C.

$\Phi_{ET}(0) = 0.06$ and $\Phi_{ET}(\infty) = 0.5$, fraction of mixing $f_m$ values were calculated from the corresponding areas under the donor decay profiles using eq 6. In Figure 4B, we plot $f_m$ as a function of annealing time. The curves have a similar shape to those in Figure 4A. At 90 °C, maximum mixing of donor and acceptor was achieved in 90 min with $\Phi_{ET}$(lim) = 0.38 and $f_m = 0.75$.

For architectural coatings, one of the most important considerations is the time scale for polymer diffusion at room temperature. In our laboratory, this is 23 °C. To emphasize that the polymer molecules in films of the P($BA_{60}$−$MMA_{39}$) latex with $T_g = 4$ °C undergo substantial diffusion at room temperature, we plot the evolution of $\Phi_{ET}$ and $f_m$ in Figure 5.

To quantitatively compare polymer diffusion rates at different temperatures, one needs to be able to compute diffusion coefficients $D$. Because there is no proper way to calculate absolute values of $D$ for mixtures of polymers of different lengths and extents and distribution of branches, we resort to a prescription that has served us well in the past: we calculate *apparent* diffusion coefficients $D_{app}$ by fitting $f_m$ data to a Fickian diffusion model.[5,11,12]

In Figure 6, values of $D_{app}$ calculated in this way for P($BA_{60}$−$MMA_{39}$) films are plotted against $f_m$ values for various annealing temperatures. At each temperature, these $D_{app}$ values decrease with increasing annealing time as slower diffusing species make their contribution to the growth in $\Phi_{ET}$. The plot also shows that the diffusion rate is faster at higher temperature for the same $f_m$ value. For example, at $f_m = 0.59$, the annealed film sample gave a value of $D_{app} = 0.007$ nm$^2$/s at 23 °C, 0.16 nm$^2$/s

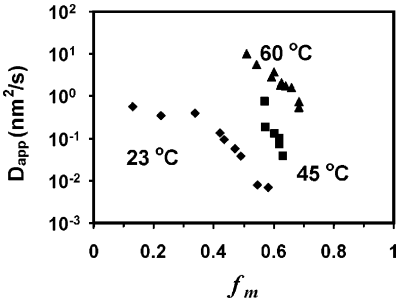


**Figure 6.** Plots of the apparent diffusion coefficient $D_{app}$ as a function of $f_m$ for P($BA_{60}$−$MMA_{39}$) latex films annealed at various temperatures.

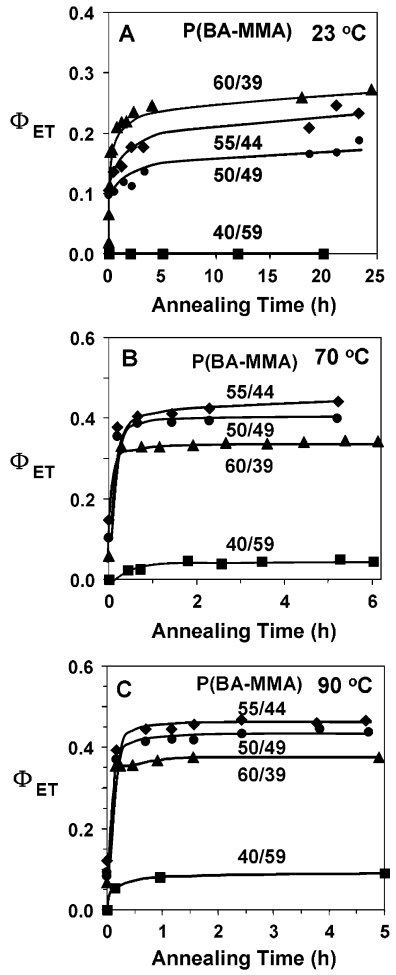


**Figure 7.** Plot of the $\Phi_{ET}$ for films formed from D/A labeled latex mixtures annealed for various periods of time at (A) 23, (B) 70, and (C) 90 °C: (▲) P($BA_{60}$−$MMA_{39}$), (◆) P($BA_{55}$−$MMA_{44}$), (●) P($BA_{50}$−$MMA_{49}$), and (■) P($BA_{40}$−$MMA_{59}$).

at 45 °C, and 4.4 nm²/s at 60 °C.

Arrhenius-type plots (ln $D_{app}$ vs $1/T$) of the data in Figure 6 are linear for $D_{app}$ values at $f_m = 0.59$. These plots are shown in Figure S1 in the Supporting Information. From the slopes of these plots, we obtained an apparent activation energy $E_a$ = 33.4 kcal/mol over the temperature range 23−60 °C. Since temperature affects the rate of diffusion by a change in the monomeric friction factor, the magnitude of $E_a$ should be independent of $f_m$. Therefore, we used this value of $E_a$ as a shift factor to create a master curve of $D_{app}$ values at 23 °C. The shifted values calculated in this way are shown in Figure 8. The success in generating the master curve serves as strong support for the validity of our analysis to obtain $D_{app}$ values.

**Polymer Diffusion in Different Composition P(BA−MMA) Films.** To compare the polymer diffusion in P(BA−MMA) latex films with various polymer compositions, we monitored the increase in $\Phi_{ET}$ for a series of latex films of each composition, each annealed at a series of temperatures. In Figure 7, these $\Phi_{ET}$ values are plotted as a function of annealing time at their corresponding temperatures. Figure 7A shows that at 23 °C three of the four latex films of different composition undergo a significant extent of diffusion on the time scale of tens of hours. The $T_g$ values of these polymer compositions range from 3 to 12 °C (Table 2), and the rate of diffusion at room temperature increases with decreasing sample $T_g$.

Only the P($BA_{40}$−$MMA_{59}$) film showed no detectable diffusion at this temperature. It has a $T_g$ slightly above room temperature, 28 °C. There are several noteworthy features of this particular set of films. When these films were cast and dried at 4 °C, well below the MFT, they were turbid and cracked. Better films for polymer diffusion studies were obtained by casting and drying at room temperature although they were still not clear and crack free due to their high MFT. Upon annealing at higher temperature, the films became more transparent, but the film became fully transparent only after it was annealed for ca. 1 h at 90 °C. Thus, dry sintering plays a role in particle coalescence in these films.[13] An increase in $\Phi_{ET}$ in these films due to polymer diffusion could be measured at 70 °C (Figure 7B). This occurred over the first hour and then appeared to cease. We speculate that this increase in $\Phi_{ET}$ is due to the contribution of diffusion of low molar mass chains in the sample. For the remainder of the experiment, polymer diffusion was very slow at this temperature but became more pronounced at 90 °C (Figure 7C).

The other samples underwent rapid polymer diffusion at 70 °C. For the P($BA_{60}$−$MMA_{39}$) film, $\Phi_{ET}$ approached $\Phi_{ET}$(lim) (0.38) in a few minutes. The P($BA_{55}$−$MMA_{44}$) and P($BA_{50}$−$MMA_{49}$) latex film samples exhibited a behavior analogous to that of the high-$T_g$ sample: rapid diffusion at early times, which appeared to level off at a $\Phi_{ET}$ value less than $\Phi_{ET}$(lim) [$\Phi_{ET}$(lim) = 0.50 for P($BA_{55}$−$MMA_{44}$) and 0.52 for P($BA_{50}$−$MMA_{49}$)]. These two films reached somewhat higher values of $\Phi_{ET}$ values when annealed for several hours at 90 °C.

It is noteworthy that $\Phi_{ET}$(lim) values for P($BA_{55}$−$MMA_{44}$) and for P($BA_{50}$−$MMA_{49}$) are higher than that for P($BA_{60}$−$MMA_{39}$) and indistinguishable from $\Phi_{ET}(\infty)$. This result suggests that there is a higher degree of branching or some undetected microgel in this P($BA_{60}$−$MMA_{39}$) sample that limits the extent to which donor- and acceptor-labeled polymers can interpenetrate.

$D_{app}$ values for these films were calculated as a function of $f_m$ at each temperature. These plots are presented in Figure 6 and Figure S2 in the Supporting Information. From Arrhenius plots of $D_{app}$ values as described above, apparent activation energies were computed. The values of $E_a$ and the temperature ranges for which they were obtained are listed in Table 3. These were then used as shift factors to create master curves of the diffusion data, as shown in Figure 8.

**Temperature Dependence of the Viscoelastic Properties of P(BA−MMA) Films.** The Williams−Landel−Ferry (WLF) equation[14] is widely employed to describe the temperature dependence of polymer diffusion using parameters obtained from viscoelastic relaxation measurements.[11,12,15] To describe polymer diffusion, the WLF equation takes the following form

$$\log (a_T) = \log\left(\frac{DT_0}{D_0T}\right) = -\frac{C_1(T - T_0)}{C_2 + T - T_0} \qquad (7)$$

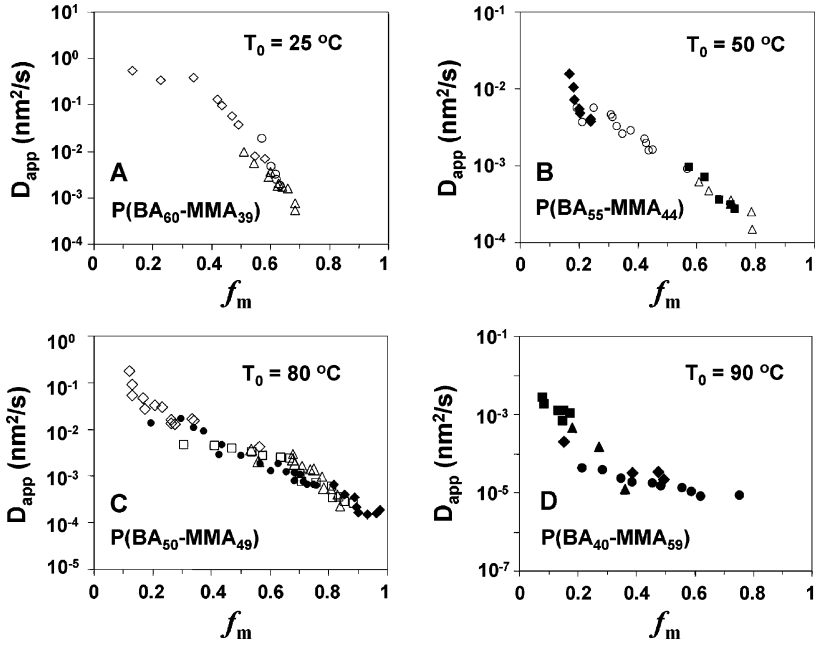


**Figure 8.** Master curves of $D_{app}$ values for (A) P($BA_{60}$−$MMA_{39}$) at 23 °C (calculated using $E_a$ = 33.4 kcal/mol as a shift factor), (B) P($BA_{55}$−$MMA_{44}$) at 23 °C (calculated using $E_a$ = 39.1 kcal/mol as a shift factor), (C) P($BA_{50}$−$MMA_{49}$) at 23 °C (calculated using $E_a$ = 45.2 kcal/mol as a shift factor), and (D) P($BA_{40}$−$MMA_{59}$) at 70 °C (calculated using $E_a$ = 64.1 kcal/mol as a shift factor).

**Table 3. $E_a$ Values of the Latex Polymers**

| | energy-transfer experiments | | rheological measurements | | | | |
|---|---|---|---|---|---|---|---|
| latex | $E_a$ (kcal/mol) | temp range (°C) | $E_a$ (kcal/mol) | temp range (°C) | $T_0$ (°C) | $C_1$ | $C_2$ (K) |
| P($BA_{60}$−$MMA_{39}$) | 33.4 | 23−60 | 28.7 | 25−70 | 25 | 10.0 | 114.9 |
| P($BA_{55}$−$MMA_{44}$) | 39.1 | 23−60 | 34.2 | 50−70 | 50 | 9.1 | 112.6 |
| P($BA_{50}$−$MMA_{49}$) | 45.2 | 23−90 | 50.3 | 80−180 | 80 | 14.2 | 107.1 |
| P($BA_{40}$−$MMA_{59}$) | 64.1 | 90−120 | 65.6 | 90−130 | 90 | 16.3 | 120.4 |

where $D_0$ is the diffusion coefficient at an arbitrary chosen reference temperature $T_0$. $C_1$ and $C_2$ are parameters that depend on the choice of the $T_0$, and they are easily transferred to other reference temperatures.

For each composition, we carried out oscillatory shear measurements as a function of frequency over a range of temperature close to that of the energy transfer experiments. Nonlabeled samples, which have similar molecular weight and PDI to dye-labeled samples (see Table 2), were used for viscoelastic measurements.

We measured the storage modulus ($G'$) and loss modulus ($G''$) as a function of frequency ($\omega$) at a series of temperatures ranging from 25 to 100 °C for P($BA_{60}$−$MMA_{39}$), from 50 to 120 °C for P($BA_{55}$−$MMA_{44}$), from 80 to 180 °C for P($BA_{50}$−$MMA_{49}$), and from 130 to 200 °C for P($BA_{40}$−$MMA_{59}$) (not shown). We used the time−temperature superposition principle (TTS) to obtain the shift factors ($a_T$) of the temperature dependence. Strictly speaking, the TTS principle can be only applied to a system in which the various relaxation times belonging to a given relaxation process have the same temperature dependence, such as linear amorphous polymers above $T_g$. P(BA−MMA) copolymer is composed of polydisperse chains with various degrees of branching.[16] It is well-known that branching may affect slightly the temperature sensitivity of the viscoelastic response, but TTS basically holds.[9,17] In Figure 9A−D, we show the $G'$ and $G''$ master curves after applying TTS, by choosing $T_0$ = 25 °C for P($BA_{60}$−$MMA_{39}$), $T_0$ = 50 °C for P($BA_{55}$−$MMA_{44}$), $T_0$ = 80 °C for P($BA_{50}$−$MMA_{49}$), and $T_0$ = 90 °C for P($BA_{40}$−$MMA_{59}$) as the reference temperatures. Only shifts in the horizontal scale were applied. Shift factors at each temperature were extracted using the generally accepted procedure of overlaying plots of tan($\delta$) ($G''/G'$) for data at different temperatures. The rheological response of all four samples is consistent with what is normally found in entangled polymer melts, in particular, that $G' > G''$ over the portion of the relaxation spectrum that is usually associated with the plateau regime. As observed in this figure, good matching between curves was obtained.

## Discussion

**Comparison between Different Experiments.** Values of the apparent activation energy in the range of temperatures studied can be obtained by plotting ln($a_T$) in Arrhenius fashion against the inverse of the absolute temperature, as empty squares shown in Figure 10. Normally the ln($a_T$) vs 1/$T$ plot is curved, but when the data are limited over a relatively narrow range of temperatures, the plot appears linear. The activation energy $E_a$ for viscoelastic relaxation can be calculated from the slope of this linear fraction of the plot. The magnitude of the $E_a$ value will increase as the measurement temperature approaches $T_g$. From Figure 10 average values of $E_a$ for each latex sample were calculated over the temperature range close to energy transfer experiments. We compare these $E_a$ values as well as their corresponding temperature ranges with those obtained from energy transfer experiments in Table 3. It can be clearly observed that the $E_a$ values from the two different methods are in good agreement when a similar temperature range was chosen.

In Figure 10, we make a direct comparison between data obtained from rheological measurements and from diffusion experiments. We plotted both data sets in the same graph, where shift factors obtained from rheology are shown as empty squares

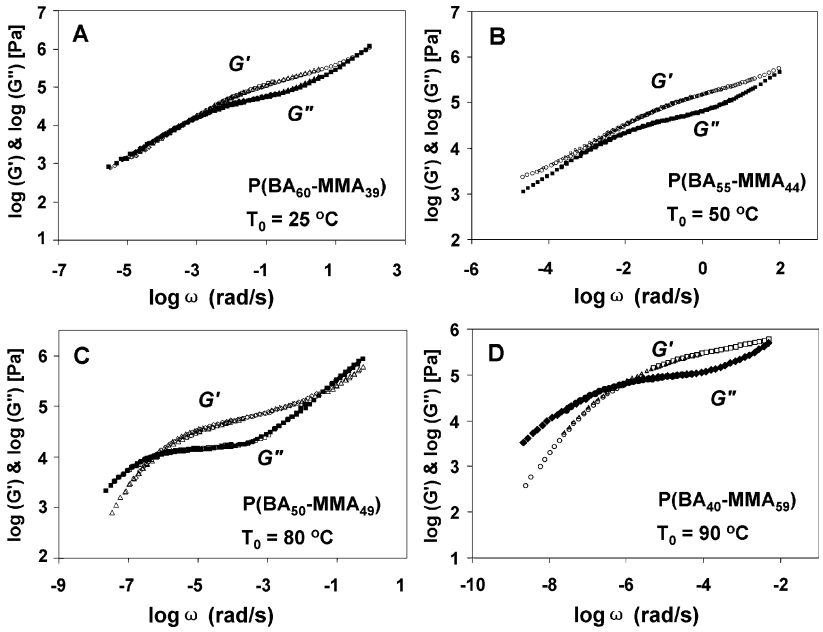


**Figure 9.** Plots of master curves of $G'$ and $G''$ for (A) P($BA_{60}$−$MMA_{39}$), (B) P($BA_{55}$−$MMA_{44}$), (C) P($BA_{50}$−$MMA_{49}$), and (D) P($BA_{40}$−$MMA_{59}$) latex films at $T_0$ = 25, 50, 80, and 90 °C, respectively.

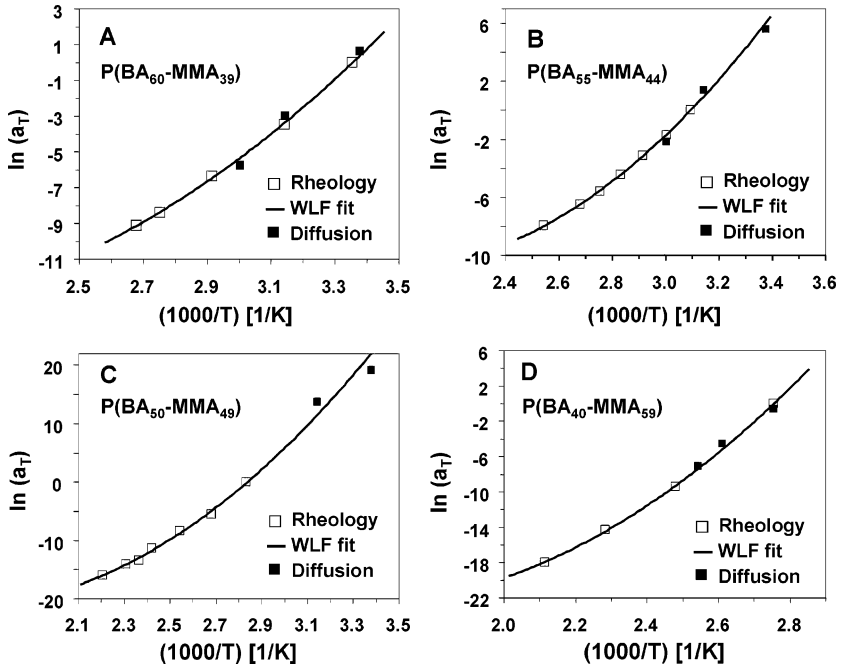


**Figure 10.** Plots of shifted $D_{app}$ and log($a_T$) against the inverse of the absolute temperatures for (A) P($BA_{60}$−$MMA_{39}$), (B) P($BA_{55}$−$MMA_{44}$), (C) P($BA_{50}$−$MMA_{49}$), and (D) P($BA_{40}$−$MMA_{59}$) latex films.

and those from the diffusion experiments are shown as filled squares. The diffusion data used in Figure 10A were taken from Figure S1 (Supporting Information) and then shifted vertically to compensate for the reference temperature. The full line represents the WLF fitting, calculated using the $C_1$ and $C_2$ listed in Table 3. Parts B−D of Figure 10 were plotted using the same process. The diffusion data and rheology data appear to track together with changing temperature.

**Effect of Long Chain Branching on the Time Dependence of $D_{app}$.** One of the striking features of our data is the time dependence of $D_{app}$. This effect is best appreciated by examining the master curves of the shifted $D_{app}$ vs $f_m$ in Figure 8. $D_{app}$ decreases by several orders of magnitude over the course of the experiment for each of the four copolymers. In Figure 8B−D, there is a sharp drop in $D_{app}$ for values of $f_m$ less than about 0.2; the high initial rate of diffusion made it impossible for us to capture the short time behavior in the P($BA_{60}$−$MMA_{39}$) sample (Figure 8A), as we could not make measurements at $f_m$ values less than 0.2 in this sample. This sharp initial drop in $D_{app}$ in Figure 8B−D is of great interest to us, and we are currently conducting experiments to determine its origin.

Our focus here is on the change in $D_{app}$ over the range in $f_m$ values from 0.2 to 0.8. For P($BA_{60}$−$MMA_{39}$), $D_{app}$ drops by about a factor of 100. For P($BA_{55}$−$MMA_{44}$), there is roughly a factor of 50−100 reduction in $D_{app}$. There is a significant amount of scatter in the data for the P($BA_{50}$−$MMA_{49}$) master curve data at $f_m$ = 0.2; taking this into account, we find that $D_{app}$ decreases over the relevant $f_m$ range by a factor of 10−50.

Again, there is scatter in the data in the P($BA_{40}$−$MMA_{59}$) master curve at $f_m = 0.2$, but we estimate an overall drop in $D_{app}$ of a factor of 5−10.

We rationalize the decrease of $D_{app}$ with increasing time in terms of the distribution of diffusion coefficients of various species in the system. We consider a simple example to illustrate how this might occur. Imagine a system consisting of two species: one with $D = 1$ nm$^2$/s and a second with $D = 0.01$ nm$^2$/s. Calculations indicate the effect of a diffusing species on the time dependence $\Phi_{ET}$ is greatly diminished once that species has diffused over some characteristic distance in the sample. The actual distance involved for a particular experiment will depend on details such as the latex particle sizes and the ratio of donor-labeled particles to acceptor-labeled particles. Assigning a number to this distance does not concern us here; the important fact is that for both species in our hypothetical sample this distance is the same. This means that in our example the slower moving species will take 100 times longer to diffuse over this characteristic distance. In an energy transfer experiment, we measure the change in $\Phi_{ET}$ vs time and convert this information into $D_{app}$ with a diffusion model.[18] Over the course of an experiment on our hypothetical system, the $D_{app}$ value extracted will be some sort of weighted average of the apparent diffusion coefficients of the two species in the system. Early in the experiment, $D_{app}$ will be weighted more heavily toward the diffusion of the faster moving species, as the motion of the faster moving species is largely what causes the change in $\Phi_{ET}$. Once the fast moving species has diffused over a characteristic distance, its contribution to the increase in energy transfer has reached its maximum value. The experiment is no longer sensitive to the faster species diffusion, and the rate of $\Phi_{ET}$ increase will drop significantly. The result of this is that the extracted $D_{app}$ value will now be weighted more heavily toward the diffusion coefficient of the slower moving species. Of course, this drop in $D_{app}$ is not expected to be sudden for the hypothetical system but instead occurs gradually.

On the basis of this argument, we suspect that the time dependence of $D_{app}$ between $f_m = 0.2$ and $f_m = 0.8$ is mostly due to a broad distribution of diffusion coefficients for polymer chains present in the sample. This breadth is apparently larger in P($BA_{60}$−$MMA_{39}$) and P($BA_{55}$−$MMA_{44}$) than it is in P($BA_{50}$−$MMA_{49}$) and P($BA_{40}$−$MMA_{59}$), based on the relative magnitudes in the change of $D_{app}$ with $f_m$. We cannot rationalize these differences in terms of sample PDI, as no trend in the PDI values in Table 2 exists. Instead, we suspect that differences in the breadth of diffusion coefficients are due to differences in the details of molecular architecture between samples. In particular, the presence of long chain branching can dramatically decrease the diffusion coefficient of a polymer;[19] a sample consisting of a range of branching architectures would be expected to have a broad distribution of diffusion coefficients and a time-dependent $D_{app}$.

It is difficult to make quantitative determinations about the relative degree of long chain branching for polymers studied here, but we can make some general qualitative comments based on the rheology data in Figure 9. The rheological responses of P($BA_{60}$−$MMA_{39}$) and P($BA_{55}$−$MMA_{44}$) are clearly quite different from P($BA_{50}$−$MMA_{49}$) and P($BA_{40}$−$MMA_{59}$). The most obvious difference is the lack of any terminal regime in the P($BA_{60}$−$MMA_{39}$) and P($BA_{55}$−$MMA_{44}$) data, despite the fact that the data is over a similar range of reduced frequencies. We believe that the differences in mechanical response between samples are due to differences in molecular architecture. We cannot help but notice that the rheological responses of P($BA_{60}$−$MMA_{39}$) and P($BA_{55}$−$MMA_{44}$) are strikingly similar to what is reported for a cross-linking polymer in the vicinity of the gel point.[20] This is not to say that P($BA_{60}$−$MMA_{39}$) and P($BA_{55}$−$MMA_{44}$) are in fact gels, but they likely share some limited structural similarities. In particular, the very broad distribution of mechanical relaxation times suggests a high degree of branching with a wide range of branch lengths. We believe that a substantial fraction of the P($BA_{60}$−$MMA_{39}$) and P($BA_{55}$−$MMA_{44}$) samples are made up of branched polymer. The data for P($BA_{50}$−$MMA_{49}$) and P($BA_{40}$−$MMA_{59}$) are quite different (Figure 9C,D) and show crossovers between $G'$ and $G''$ in the interval between the rubbery zone and the terminal zone of the master curve. This response is typical for linear polymers of unimodal molecular weight distributions of moderate PDI and is anticipated by theory.[21] Solely on the basis of the rheological response of P($BA_{50}$−$MMA_{49}$) and P($BA_{40}$−$MMA_{59}$), we suspect that chains with significant degrees of long chain branching make up a relatively small amount of the overall population of chains in the system.

It is well-established that chain transfer to polymer often produces highly branched structures in the emulsion polymerization of butyl acrylate.[22,23] This is consistent with what we infer from rheology experiments, where evidence suggests that a greater degree of long chain branching is present in P($BA_{60}$−$MMA_{39}$) and P($BA_{55}$−$MMA_{44}$). This accounts for the broader distribution of diffusion coefficients in these samples that is inferred from the time dependence of $D_{app}$.

An alternate explanation for the time dependence of $D_{app}$ in energy-transfer experiments has been advanced by O'Neil and Torkelson.[24] They propose that ignoring interchain correlation effects (i.e., "correlation hole" effects)[25] in the energy transfer model for polymer diffusion can lead to the erroneous conclusion that $D_{app}$ decreases with increasing $f_m$. While we accept this possibility in principle, we believe that this effect is not the primary source of the change of $D_{app}$ with $f_m$ shown in Figure 8. We base this belief on two things. First, according to O'Neil and Torkelson's calculations, $D_{app}$ is nearly constant until $f_m > 0.8$. We have restricted our analysis to $f_m$ values less than 0.8; the change in $D_{app}$ occurs over the entire range of $f_m$. Second, the magnitude in the decrease of $D_{app}$ in O'Neil and Torkelson's calculations is relatively small; up to $f_m = 0.9$ they only report a factor of 2 decrease in the calculated $D_{app}$. Of course, their results are for a system that is somewhat different from ours—their model treats linear chains with a single donor or acceptor label at one end. Still, it is hard to rationalize that merely changing the labeling scheme could have such a big effect so as to account for the results in Figure 8.

## Summary

We synthesized donor- and acceptor-labeled P(BA−MMA) copolymer latex particles by semicontinuous emulsion polymerization in the presence of 0.25 wt % $C_{12}$-SH. Four sets of copolymers were prepared from various weight ratios of BA and MMA. Weight ratios of BA:MMA:MAA for these latexes are 60:39:1, 55:44:1, 50:49:1, and 40:59:1. Their glass transition temperatures ($T_g$) are 4, 7, 12, and 28 °C, respectively. Donor-labeled latex samples were prepared in the presence of 1 mol % of PheMMA as the dye-containing comonomer. Acceptor-labeled latex samples were prepared in the presence of 0.3 mol % of NBenMA. The latex particles had diameters of ca. 150 nm with narrow size distribution. FRET experiments were used to determine the apparent polymer diffusion coefficients as a function of temperature for each of the latex samples.

Analysis of the diffusion data gave apparent activation energy $E_a$ values of ca. 33 kcal/mol for P($BA_{60}$−$MMA_{39}$), 39 kcal/

mol for P($BA_{55}$−$MMA_{44}$), 45 kcal/mol for P($BA_{50}$−$MMA_{49}$), and 64 kcal/mol for P($BA_{40}$−$MMA_{59}$). The temperature dependence of the polymer diffusion coefficients closely matches the temperature dependence extracted from a master curve analysis of the rheology data for each latex. The rheology data lead us to conclude that latex polymers with increasing BA content have a greater degree of long-chain branching. Differences in long-chain branching also show up in the diffusion measurements, which indicate a larger distribution of polymer diffusion coefficients in samples with higher BA content. These results will guide the development of the next generation of low VOC coatings.

**Acknowledgment.** The authors thank Rohm & Haas, Rohm and Haas Canada, and NSERC Canada for their support of this research. Y.L. thanks Materials and Manufacturing Ontario (MMO) for a scholarship and expresses his appreciation to Dr. Zhihui Yin for valuable discussions.

**Supporting Information Available:** A plot of ln $D_{app}$ vs $1/T$ for P($BA_{60}$−$MMA_{39}$) and plots of log $D_{app}$ vs $f_m$ for all samples examined, as well as GPC traces for a NBen-labeled polymer, and a description of the determination of the Förster radius for Phe and NBen. This material is available free of charge via the Internet at http://pubs.acs.org.

## References and Notes

(1) Bezinski, J. J. Regulation of Volatile Organic Compound Emission from Paints and Coatings. In *Paint and Coating Testing Manual: Fourteenth Edition of the Gardner-Sward Handbook*; Koleske, J. V., Ed.; 1995.
(2) Paton, T. C. *Paint Flow and Pigment Technology*; Wiley: New York, 1979.
(3) Zhao, C. L.; Wang, Y.; Hruska, Z.; Winnik, M. A. *Macromolecules* **1990**, *23*, 4082−4087.
(4) Oh, J. K.; Wu, J.; Winnik, M. A.; Craun, G. P.; Rademacher, J.; Farwaha, R. *J. Polym. Sci., Part A: Polym. Chem.* **2002**, *40*, 1594−1607.
(5) Oh, J. K.; Wu, J.; Winnik, M. A.; Craun, G. P.; Rademacher, J.; Farwaha, R. *J. Polym. Sci., Part A: Polym. Chem.* **2002**, *40*, 3001−3011.
(6) Tronc, F.; Liu, R.; Winnik, M. A.; Eckersley, S. T.; Rose, G. D.; Weishuhn, J. M.; Meunier, D. M. *J. Polym. Sci., Part A: Polym. Chem.* **2002**, *40*, 2609−2625.
(7) O'Connor, D. V.; Phillips, D. *Time-Correlated Single Photon Counting;* Academic Press: New York, 1984.
(8) James, D. R.; Demmer, D. R. M.; Verrall, R. E.; Steer, R. P. *Rev. Sci. Instrum.* **1983**, *54*, 1121−1130.
(9) Bartels, C. R.; Buckley, C.; Graessley, W. W. *Macromolecules* **1984**, *17*, 2702−2708.
(10) Lakowicz, J. R. *Principles of Fluorescence Spectroscopy*; Plenum: New York, 1983.
(11) Wu, J.; Tomba, J. P.; Winnik, M. A.; Farwaha, R.; Rademacher, J. *Macromolecules* **2004**, *37*, 2299−2306.
(12) Oh, J. K.; Tomba, J. P.; Ye, X.; Eley, R.; Rademacher, J.; Farwaha, R.; Winnik, M. A. *Macromolecules* **2003**, *36*, 5804−5814.
(13) Sperry, P. R.; Snyder, B. S.; O'Dowd, M. L.; Lesko, P. M. *Langmuir* **1994**, *10*, 2619−2628.
(14) Ferry, J. D. *Viscoelastic Properties of Polymers*; Wiley: New York, 1980.
(15) Nemoto, N.; Landry, M. R.; Noh, I.; Yu, H. *Polym. Commun.* **1984**, *25*, 141.
(16) Wu, J.; Oh, J. K.; Yang, J.; Winnik, M. A.; Farwaha, R.; Rademacher, J. *Macromolecules* **2003**, *36*, 8139−8147.
(17) Carella, J. M.; Gotro, J. T.; Graessley, W. W. *Macromolecules* **1986**, *19*, 659−667.
(18) Wang, Y.; Zhao, C.-L.; Winnik, M. A. *J. Chem. Phys.* **1991**, *95*, 2143−2153.
(19) McLeish, T. C. B. *Adv. Phys.* **2002**, *51*, 1379−1527.
(20) Winter, H. H.; Chambon, F. *J. Rheol.* **1986**, *30*, 367−382.
(21) Wasserman, S. H.; Graessley, W. W. *J. Rheol.* **1992**, *36*, 543−572.
(22) Former, C.; Castro, J.; Fellows, C. M.; Tanner, R. I.; Gilbert, R. G. *J. Polym. Sci., Part A: Polym. Chem.* **2002**, *40*, 3335−3349.
(23) Gonzalez, I.; Leiza, J. R.; Asua, J. M. *Macromolecules* **2006**, *39*, 5015−5020.
(24) O'Neil, G. A.; Torkelson, J. M. *Macromol. Theory Simul.* **1997**, *6*, 931−948.
(25) de Gennes, P.-G. *Scaling Concepts in Polymer Physics;* Cornell University Press: Ithaca, NY, 1979.

MA070853C